# Characterization of Intra-platoon V2V Links in Long Homogeneous Platoons

Saeid Sabamoniri*, Pedro M. Santos†, Luis Almeida‡
* *CISTER Research Unit / Universidade do Porto – Faculdade de Engenharia – Portugal*
† *CISTER Research Unit & Universidade de Aveiro – Departamento de Eletrónica, Telecomunicações e Informática – Portugal*
‡ *Universidade do Porto – Faculdade de Engenharia – Portugal*
ssmon@isep.ipp.pt, pss@ua.pt, lda@fe.up.pt

***Abstract*—Vehicular platooning aims to improve fuel efficiency and traffic fluidity, and wireless protocols can support such goals. Platoons benefit all vehicle classes (e.g., passenger, truck, trailer), and can be made arbitrarily long, to the extent control and networking mechanisms allow. Vehicle-to-Vehicle (V2V) wireless links inside the platoon are susceptible to path loss, shadowing & diffraction by vehicular obstacles, and fading. In this paper we characterize V2V intra-platoon links at the physical and data-link levels, for platoons composed of same-class vehicles. Our simulation results, using a 30 vehicle-long platoon, show that vehicle dimensions affect propagation and link-level performance, notably that Packet Delivery Ratio (PDR) for edge nodes in an all-passenger vehicle scenario can be 3 times higher than for an all-trailer scenario.**

***Index Terms*—ITS, vehicular communication, wireless signal propagation, wireless communication obstacles.**

## I. Introduction

Autonomous vehicles with a high or full automation level are expected to compose about 14% of all light vehicle sales by 2040 [1]. Pairing autonomous driving with wireless connectivity produces Cooperative Autonomous Vehicles (CAV), that enables cooperation and coordination towards e.g. improved safety and fuel consumption. Such advancements will impact all classes of road vehicles, such as passenger, truck or trailer vehicles. We focus on a particular CAV application, platooning, in which a string of (wireless-enabled) vehicles travels with short inter-vehicle distance. Platooning allows fuel efficiency gains due to slipstream, but it imposes stringent requirements on reaction time of vehicles, and therefore on the communication system. One can envision that, over long distances, **long** platoons can emerge for efficiency purposes, as vehicles entering and leaving the platoon at their discretion. There is no concrete number as to when a platoon becomes *long*, but we offer two criteria. 1) **From a control perspective:** the number of elements is such that the need for *local* control mechanisms arises within the platoon. 2) **From a connectivity perspective:** the number of elements is such that a direct link between the edge vehicles becomes unlikely.

This work was supported by national funds through FCT/MECI (Portuguese Foundation for Science and Technology), within the CISTER Research Unit (UIDP/UIDB/04234/2020) and under the project Intelligent Systems Associate Laboratory - LASI (LA/P/0104/2020), and Route 25 (ref. TRB/2022/00061 - C645463824-00000063), funded by the EU/Next Generation, within call n.º 02/C05-i01/2022 of the Recovery and Resilience Plan (RRP). The work of Saeid Sabamoniri is supported by a Ph.D. Scholarship from FCT, grant nr. 2023.00896.BD.


Fig. 1: Long platoon (passenger vehicle scenario) and communication impairment (shown specifically for leader).

Our work aims to help answer the question from the *connectivity perspective*. The challenge in this context is that wireless messages broadcast by the platoon leader, typically the front vehicle, no longer reach all platoon members (Fig. 1). Past works such as LHP [2] and L-Platooning [3] propose wireless protocols that integrate with the vehicles' control systems to support such long platoons. To handle communication impairments due to path loss and vehicle obstruction, both works propose the breakdown into sub-platoons, whose leaders relay messages to platoon members located farther away.

Evaluating the performance of such protocols requires accurate characterization of the intra-platoon vehicle-to-vehicle (V2V) propagation. Modelling V2V links with vehicles in-between must include long-distance path loss and stochastic fading models, as well as models to account for the impact of obstacles in the received signal. Several works have measured the impact of vehicular obstructions in outdoor experimental campaigns. The authors of [4], measuring in a highway scenario, report signal attenuation by obstructions can reach up to ∼10dB w.r.t. line-of-sight (LoS), and varies with the dimensions of the obstructing vehicle. In [5], the impact of non-LoS conditions during day/night times on RSSI and PDR is evaluated. The authors conclude that, at close distances, vehicular obstacles cause significant attenuation on signal power. To model the impact of vehicular obstructions, the authors of [6] used Fresnel zones and the knife-edge model. This approach has been used in the vehicular networking simulator VEINS [7], which we use for our characterization.

In this paper, we aim to accurately characterize V2V links in long platoons, where all vehicles pertain to one of three classes: Passenger, Trucks and Trailers. The characterization is made in terms of PDR, Received Signal Strength (RSS), and Inter-Arrival Time (IAT). We used well-established simulation tools (VEINS and SUMO [8], a mobility simulator), and include accurate propagation modeling, namely by accounting the impact of vehicles between Tx and Rx. Our results show better connectivity (PDR) at the center of the platoon, for all considered vehicle

types, and that propagation and data-link performance degrades as vehicle dimensions increase. PDR experienced by Passenger vehicles can be triple of that observed by Trailers.

Our contributions are: (i) focus on a long platoon scenario (most measurement campaigns look into small-scale scenarios [4], [5]); (ii) accurate propagation modelling, often unnaccounted for in literature (e.g., [3] considers only PDR); (iii) experimental (simulation-based) characterization of expected performance.

This document is structured as follows. Sec. II describes the adopted propagation models. Simulation setup is described in Sec. III, and experimental results are presented in Sec. IV. Final remarks are drawn in Sec. V.

## II. Propagation Modelling

We address **homogeneous** platoons, i.e., platoons are composed of vehicles of the same class. Their dimensions of the three classes considered (Passenger, Trucks and Trailers) are described in Table I. Wireless antennas are placed on the top and front edge of the vehicles and have a height of 10cm.

### A. Path Loss Model

The Free Space Path Loss (FSPL) [9] is a well-established and validated large-scale propagation model derived from physical properties to model received power as a function of distance $d$ between Tx and Rx in LoS scenarios. It follows Eq. 1 where $P_t$ is the transmit power and $\lambda$ the wavelength.

$$FSPL = \frac{P_t \lambda^2}{16\pi^2 d^2} \tag{1}$$

We refrain from using the Two-Ray Ground-Reflection Model, that accounts for the impact of a signal copy reflected on a relevant surface (typically the ground). In our scenario, the ground as reflective surface is only relevant for immediate neighbors; the predominant reflective surfaces are the vehicle rooftops. Even so, this surface is not present for all possible links. Consider that, for Rx and Tx of similar height, the reflection point occurs at mid-distance. In an (idealized) representation of a platoon, the reflection point to a receiver one car away will be the rooftop of the in-between car; but to a receiver two cars away, the reflection point will fall on the ground. We recognize the relevance of this propagation phenomena but, due to its circumstantial nature, we leave its study to future work.

### B. Attenuation by Obstacles

*1) Fresnel Zone & Knife-Edge Model:* The impact in the propagated signal of obstacles (in our scenario, other platoon members) between transmitter and receiver can be modeled by Fresnel zones. The Fresnel zone (of ellipsoid shape) models signal copies that can follow slightly different paths between Tx and Rx, especially caused by obstructions or deflecting objects. More concretely, Fresnel zones represent successive regions where secondary waves have a path length from Tx to Rx $n\lambda/2$ greater than the total path length of a LoS path [9]. The radius of the $n^{\text{th}}$ Fresnel ellipsoid is denoted by $r_n$, and it can be expressed by Eq. 2:

$$r_n = \sqrt{\frac{n\lambda d_1 d_2}{d_1 + d_2}} \tag{2}$$

where $\lambda$ is the wavelength, $d_1$ and $d_2$ are the distances to the obstacle from the transmitter and receiver. Eq. 2 provides the ellipsoid's radius at the distance $d_1$ between Tx and obstacle; setting $d_1 = d_2$ outputs the largest ellipsoid's radius. The Fresnel radius is used in a dimensionless parameter normally denoted by $\nu$ and described by Eq. 3:

$$\nu = \frac{\sqrt{2}H}{r_1} \tag{3}$$

where $r_1$ is the radius of the first Fresnel zone and $H$ the height difference between obstacle and LoS. Following [9], the guideline for LoS microwave links is that, as long as 55% of the first Fresnel zone is kept clear, then further Fresnel zone clearance does not significantly alter loss.

Attenuation induced by individual obstacles can be modeled by the knife-edge model. The obstacle is represented as a knife-edge (specifically, a semi-infinite perfectly absorbing plane placed perpendicular to the radio link between Tx and Rx) that *intrudes* the ($1^{\text{st}}$) Fresnel zone. Based on the Huygens principle, the electric field is the sum of Huygens sources located in the plane above the obstruction and can be computed by solving the Fresnel integrals [6]. In this context, the parameter $\nu$ quantifies (indirectly) the scale of the knife-edge *intrusion* into the Fresnel zone. Following [10], the additional attenuation (in dB) due to a single knife-edge obstacle $A_{\text{sk}}$ can be approximated by:

$$\mathrm{A_{sk}} = \begin{cases} 0, & \text{if } \nu \leq -0.7 \\ 6.9 + 20\log_{10}\left(\sqrt{(\nu-0.1)^2+1} + \nu - 0.1\right), & \text{otherwise} \end{cases} \tag{4}$$

*2) Multiple Knife-Edge:* The propagation path may consist of more than one obstruction, in which case the total diffraction loss due to all obstacles must be computed. The extension of the single knife-edge obstacle case to the multiple knife-edge is not immediate. We select as reference the ITU-R method [10], that has been used in the literature (e.g., [6]) and is implemented (to the extent we could determine) by the VEINS library. In this method, vehicle obstacles between transmitter and receiver are modeled as multiple isolated cylinders, and a modified version of the Epstein-Patterson method (described in [10, Sec.4.4]) is applied. The first step is to perform a *rope-stretching* analysis of the profile, i.e., identify all relevant profile points between transmitter and receiver. Then, attenuation induced by multiple knife-edge obstacles can be approximated by their straightforward addition: $A_{\text{mk}} = \sum_{i=1}^{N} A_{\text{sk}_i}$. If (most) obstacles are taller than the LoS, some obstacles may be ignored if they are not taller than nearby obstacles; and several correcting factors must be added for a better estimate. In our scenario, all obstacles are below the LoS, so we exclude the correcting factors.

### C. Nakagami Fading

The received signal is subject to significant small-scale signal fading. The most popular model used for this purpose is the Nakagami fading model [11]. The received power $P_r$ follows a Gamma distribution with shape parameter $m$ (also referred to as the fading parameter) and scale parameter $\Omega_p/m$. The resulting probability density function is described by Eq.5 where $\Gamma(\cdot)$

TABLE I: Simulation setup details for vehicles.

| Parameter Name | Passenger | Truck | Trailer |
|---|---|---|---|
| Length | 4m | 7.1m | 16.5m |
| Width | 1.8m | 2.4m | 2.55m |
| Height | 1.5m | 2.4m | 4m |
| Inter-vehicle distance | 2m | 4.5m | 4.5m |
| Transmitted packets | 523 | 271 | 327 |
| Maximum receivable packets /node | 15164 | 7855 | 9478 |
| Min. Fresnel radius (m) w.r.t. V0 | 0.295 | 0.431 | 0.454 |
| Max. Fresnel radius (m) w.r.t. V0 | 0.317 | 0.475 | 0.477 |

denotes the Gamma function and $\Omega_p$ the mean received power, computed from a path loss model.

$$p(P_r) = \frac{m}{\Omega_p \Gamma(m)} \left( \frac{mP_r}{\Omega_p} \right)^{m-1} e^{-mP_r/\Omega_p}, \quad (5)$$

The Nakagami model is able to express different severities of fading. If $m=1$, the model maps into Rayleigh fading; if $m>1$, Rician fading with parameter $K$ is closely approximated by $m=\frac{(K+1)^2}{2K+1}$; and if $m\to\infty$, no fading is applied.

## III. Experimental Setup

We characterize the intra-platoon V2V links in a highway scenario, in static conditions (vehicles are stopped at a fixed distance from each other) and in the absence of any other traffic. We used SUMO [8], a microscopic mobility simulator, and OMNeT++ [12], a network simulator, coupled with vehicular networking library VEINS [7] and PLEXE [13], a framework to simulate the control and connectivity of platoons.

We handle each vehicle class in a separate scenario; i.e., in a given scenario, all vehicles are of the same class and have the same physical dimensions (see Table I). We use 30 vehicle-platoons in all scenarios, following related literature [3]. IEEE802.11p radios are used for the V2V communications (operating at 5.9 GHz), and On-Board Units broadcast 5 beacons per second. We use 10 cm monopole antennas placed in the front edge of the vehicle's rooftop, radiating isotropically in the horizontal plane. Transmission power is 20mW; the lower power (w.r.t. legal maximum of 100mW) is a typical strategy for intra-platoon communications, to minimize impact and interference on external (wireless) traffic. Minimum detectable power is -94 dBm, i.e., signals with power inferior to this threshold are not detected. The implementation of the propagation models described in Sec. II is the one available in the VEINS framework, under *Analogue Models* [14] : (Free-Space) `Simple Path Loss`, `Vehicle Obstacle Shadowing`, and `Nakagami Fading`. All these models are composed additively. There are no environmental elements introducing reflections and shadowing apart from ground and platoon vehicles.

The data collection period of the simulation is 105, 54, and 65 seconds for the Passenger, Truck, and Trailer scenarios, respectively. Results are expressed as percentage to abstract the different simulation times. We log and process wireless messages to produce these results. Packet loss can be caused by bit errors due to low power, insufficient power for detection, collision and interference. A collision loss refers to a packet being received that suffers bit errors due to another incoming packet that degraded Signal-to-Interference-plus-Noise Ratio (SINR). The incoming packet is counted as interference.

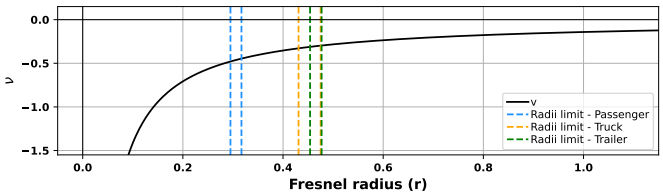


Fig. 2: $\nu$ as a function of Fresnel radius (see Eq. 3). The smallest and largest Fresnel radii are shown for the various vehicle classes (L and R respectively). All $\nu$ values are larger than threshold -0.7, implying attenuation (see Eq. 4).

*1) Vehicle Obstacle Modelling & VEINS Implementation:* On average, the distance between vehicle antennas is about 6 m for the Passenger vehicle scenario, 11.6 m for the Truck scenario, and 21 m for the Trailer scenario. Using this data and taking as reference the leader vehicle (V0), we compute the inter-antenna distance to the closest and farthest neighbor with obstacle in-between (V2 and V29 respectively). We then compute the corresponding Fresnel radius at the distance of the **first** obstacle from Tx (smallest for the V0-V2 link, largest for the V0-V29 link); these are shown in Table I. We consider only the first obstacle as, in our scenario, *all* obstacles have the same height, and the impact of subsequent obstacles is residual. We present the value of $\nu$ as a function of Fresnel radius in Fig. 2, and also depict in (vertical lines) the smallest and largest Fresnel radius at the distance of the first obstacle with respect to the leader. This confirms, following Eq. 4, that the (first) obstacle introduces attenuation in the links from V0 to any other platoon member.

The implementation of vehicular attenuation in VEINS is named `Vehicle Obstacle Shadowing` (VOS). The VOS implementation represents vehicles as bounding boxes; at each packet transmission, it identifies all obstacle vehicles intersecting the direct line connecting Tx and Rx. For each obstacle identified, the corresponding Fresnel radius and $\nu$ parameter are computed using Eq. 2 and 3 respectively. The Tx and Rx height used for the Fresnel radius computation is the sum of the vehicle height plus the antenna height. The implementation applies Eq. 4 to compute the attenuation induced by each obstacle. In more detail, the implementation represents the lateral height profile of the link using the *rope-stretching* algorithm mentioned in Sec. II-B to learn which obstacles interfere with the LoS. If an obstacle obstructs the LoS, additional correction factors are applied to refine the estimate of the obstacle's attenuation. In our scenario, all the vehicles have the same height and do not obstruct LoS, so no correction factors are applied; and the VOS implementation considers attenuation to be caused solely by the vehicle closest to the transmitter.

## IV. Link Characterization

### A. Received Signal Strength (RSS)

We plot the RSS from the perspective of three platoon vehicles: the front-leader vehicle (V0), the last vehicle (V29), and one vehicle at mid-platoon (V14). Fig. 3 shows boxplots of RSS per packet as received by the leader vehicle for the various classes of

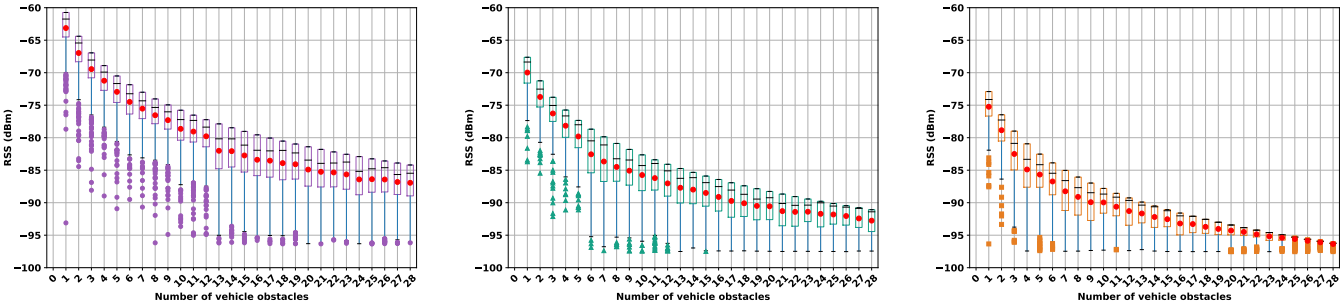


((a)) Passenger scenario; leader vehicle. ((b)) Truck scenario; leader vehicle. ((c)) Trailer scenario; leader vehicle.

Fig. 3: Boxplots of received signal strength per packet in dBm vs. number of obstacles. Not detectable packets are included.

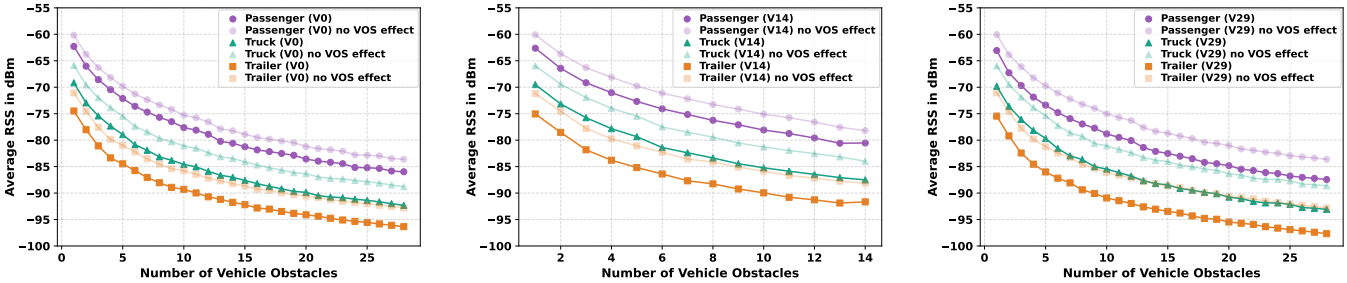


((a)) Leader vehicle of different scenarios. ((b)) The middle vehicle of different scenarios. ((c)) The last vehicle of different scenarios.

Fig. 4: Average RSS for leader (V0), middle (V14), and last vehicles (V29) vs. number of in-between vehicles.

vehicles (Passenger, Truck and Trailer respectively). We observe that RSS decreases more aggressively as the vehicle dimensions increase. This is explained mostly by the larger inter-antenna distance that occurs as we move from Passenger, to Truck, and to Trailer scenario. The immediate impact is on path loss. Focusing on the leader (Fig. 3(a)), for the Passenger scenario, the Free-Space Path Loss model predicts an RSS of -60dBm for the immediate neighbour (antennas apart by 6m), and of -71dBm for the Trailer scenario. Albeit not clearly visible, obstacle-induced attenuation occurs in all scenarios; all present values of $\nu$ (Eq. 3) are superior to the critical threshold of -0.7 (Eq. 4), for which knife-edge attenuation is applied. The impact of Nakagami fading is visible in all plots. The $4^{\text{th}}$ quartile of RSS samples (Fig. 3) expresses itself around the value produced by the FSPL and VOS models; the following 50% samples ($3^{\text{rd}}$ and $2^{\text{nd}}$ quartiles) occur within a window of $\sim$10 dB; and the remainder extends until low signal power values. Red points in each sample of Fig. 3 illustrate the average values to facilitate the comparison with Fig. 4.

We provide additional insight on the impact of the VOS model. Fig. 4 displays the average strength of received signals by three selected vehicles for the vehicle classes: the leader, V0 (Fig. 4(a)); a vehicle in the middle of the platoon, V14 (Fig. 4(b)); and the tail vehicle, V29 (Fig. 4(c)). We plot the RSS including and excluding the impact of the VOS model. We observe that VOS-induced attenuation increases as vehicle dimensions increase. This is to be expected. Larger inter-antenna distances lead to larger Fresnel radii and, following Eq. 3, the dimensionless parameter $\nu$ becomes smaller. The value of the obstacle attenuation $A_{\text{sk}}$ tends to increases as $\nu$ increases (until some point).

### B. Packet Delivery Ratio (PDR) & Link Characteristics

PDR is the ratio between the number of successfully received packets for a vehicle and the number of packets created and transmitted by the sender vehicle ($PDR = \frac{N_{Rec}}{N_{Tran}} * 100$). Fig. 5(a) reports PDR for all three scenarios. Note that distances between vehicles are different for each vehicle class; this is shown on the top of the graph. We observe that PDR decreases towards at the edges of the platoon; and as vehicle dimensions increase. Focusing on V29, the vehicle in the all-passenger vehicle scenario observes 83.4% PDR, whereas for the all-trailer scenario this value is of only 25.2%. This amounts to a more than **3-fold** difference in PDR.

Packet losses are classified into: (i) bit errors, (ii) insufficient signal power, (iii) collision, and (iv) interference by sending another packet. Fig. 5(b) presents the ratio of packets lost due to bit errors, and Fig. 5(c) shows the ratio of packets not detected due insufficient power in the received signal. Conversely to PDR, both ratios increase towards the edges and as dimensions increase. For the largest vehicles (Trailers), there is a consistent ratio of packets lost to bit errors across the whole platoon. Fig. 5(d) illustrates the collision rate, and Fig. 5(e) shows the rate of packets that experienced interference. These metrics account for residual losses, and have higher incidence as vehicle dimensions are larger.

### C. Inter-Arrival Time (IAT)

The inter-arrival time (IAT) shows the time interval between two consecutive packets received in a vehicle. IAT is particularly important for applications with temporal requirements regarding communications, for example safety-related control apps, such as the one described in [2]. In our scenario, each vehicle transmits a packet in each 200 miliseconds, or 5 packets in each

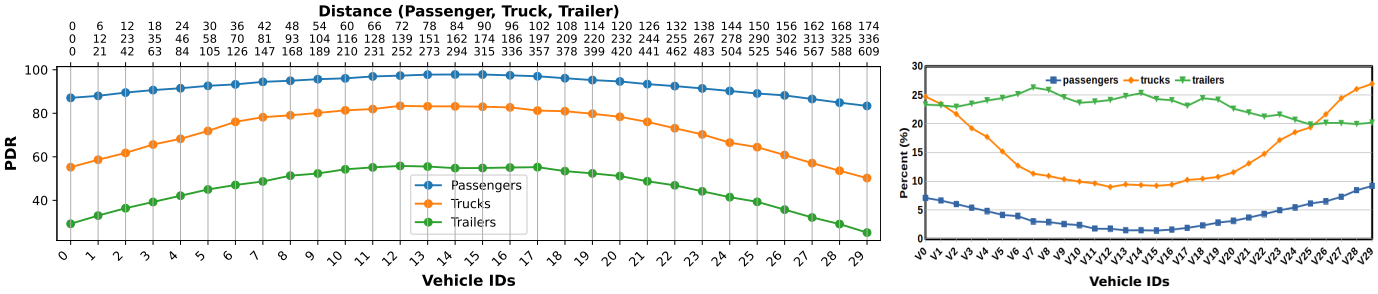


((a)) PDR for the three scenarios.

((b)) Ratio of packets lost to bit errors.

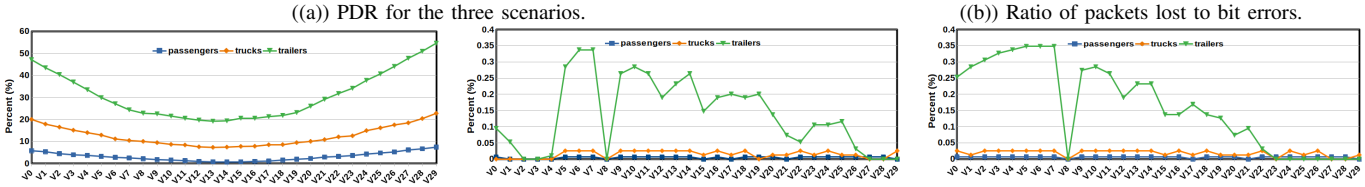


((c)) Ratio of packets not detected.

((d)) Ratio of packets lost to collision.

((e)) Ratio of packets lost to interference.

Fig. 5: Statistics for delivered, lost, and attenuated packets in each scenario.

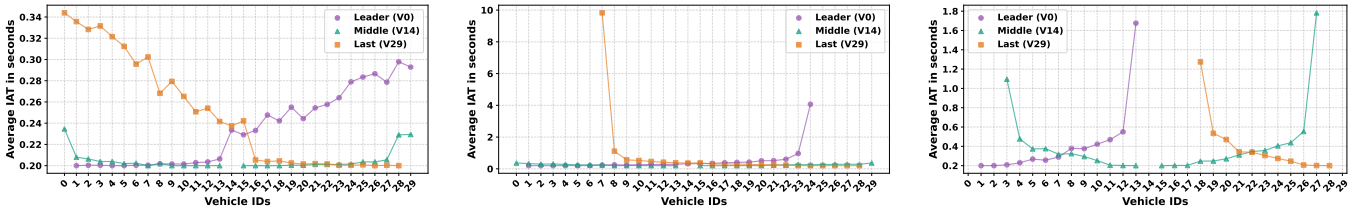


((a)) Passenger scenario.

((b)) Truck scenario.

((c)) Trailer scenario.

Fig. 6: Average IAT in each platooning scenario.

second (Sec. III). Retrasmissions and complete failure to get a packet across lead to increased IAT values. Fig. 6 shows the average IAT values for three vehicles (leader, middle, and last vehicle) in each vehicle class scenario. We observe symmetrical curves for the leader (V0) and tail vehicle (V29): packets received from closest neighbors present IAT close to nominal (200ms), and then increases as transmitter vehicle are located at the platoon middle and further. The middle vehicle (V14) observes symmetrical IAT patterns in links forth and back. The Truck and Trailer scenarios exhibit similar behaviors, accounting for inferior reception ranges (in terms of number of in-between vehicles). This leads IAT values to rise closer to the range.

## V. Conclusion

We report physical and data-link layer metrics of performance for V2V links internal to vehicular platoons, that are composed of vehicles of the same type (Passenger, Truck or Trailer). We include in our propagation modelling path loss, fading and the impact of vehicular obstacles – the platoon members themselves – through the Fresnel ellipsoid and knife-edge models. Results show that impairments in RSS, PDR and IAT are to be expected, and that these aggravate as vehicle dimensions increase. Longer distances impose larger path loss signal attenuation, but obstructions are also involved. In our modeling, longer distances mean longer Fresnel zones, thus larger Fresnel radius, and ultimately larger attenuation. Future work involves including the two-ray reflection model, extend the work to heterogeneous platoons (platoons composed of vehicles of different classes), and carrying out measurement campaigns to validate the presented findings.

## References


[1] Goldman Sachs. (2024) Partially autonomous cars forecast to comprise 10% of new vehicle sales by 2030. [Online]. Available: https://www.goldmansachs.com/insights/articles/partially-autonomous-cars-forecast-to-comprise-10-percent-of-new-vehicle-sales-by-2030

[2] S. Sabamoniri, P. M. Santos, and L. Almeida, "An ETSI ITS-Compliant Formation Protocol to Support Long Heterogeneous Platoons," in *IEEE Vehicular Networking Conference (VNC)*, 2023, pp. 53–56.

[3] M. Won, "L-platooning: A protocol for managing a long platoon with dsrc," *IEEE Trans. on Intelligent Transportation Systems*, vol. 23, no. 6, pp. 5777–5790, 2022.

[4] M. Segata, B. Bloessl, S. Joerer, C. Sommer, R. Lo Cigno, and F. Dressler, "Short paper: Vehicle shadowing distribution depends on vehicle type: Results of an experimental study," in *2013 IEEE Vehicular Networking Conference*, 2013, pp. 242–245.

[5] R. Meireles, M. Boban, P. Steenkiste, O. Tonguz, and J. Barros, "Experimental study on the impact of vehicular obstructions in vanets," in *2010 IEEE Vehicular Networking Conference*, 2010, pp. 338–345.

[6] M. Boban, T. T. V. Vinhoza, M. Ferreira, J. Barros, and O. K. Tonguz, "Impact of vehicles as obstacles in vehicular ad hoc networks," *IEEE Journal on Selected Areas in Comm.s*, vol. 29, no. 1, pp. 15–28, 2011.

[7] C. Sommer, R. German, and F. Dressler, "Bidirectionally Coupled Network and Road Traffic Simulation for Improved IVC Analysis," *IEEE Trans. on Mobile Computing*, vol. 10, no. 1, pp. 3–15, January 2011.

[8] P. A. Lopez, M. Behrisch, L. Bieker-Walz, J. Erdmann, Y.-P. Flötteröd, R. Hilbrich, L. Lücken, J. Rummel, P. Wagner, and E. Wießner, "Microscopic traffic simulation using sumo," in *The 21st IEEE Int'l Conf. on Intelligent Transportation Systems*. IEEE, 2018.

[9] T. Rappaport, *Wireless Communications: Principles and Practice*, 2nd ed. USA: Prentice Hall PTR, 2001.

[10] I. T. Union, "Propagation by diffraction," *Rec. ITU-R P. 526-14*, 2018.

[11] H. Schumacher and H. Tchouankem, "Highway propagation modeling in vanets and its impact on performance evaluation," in *Conference on Wireless On-demand Network Systems and Services (WONS)*, 2013, pp. 178–185.
[12] A. Varga and R. Hornig, "An overview of the omnet++ simulation environment," in *Int'l Conf. on Simulation Tools and Techniques (ICST)*, 2008.
[13] M. Segata, R. Lo Cigno, T. Hardes, J. Heinovski, M. Schettler, B. Bloessl, C. Sommer, and F. Dressler, "Multi-Technology Cooperative Driving: An Analysis Based on PLEXE," *IEEE Transactions on Mobile Computing*, vol. 22, no. 8, pp. 4792–4806, 8 2023.
[14] C. Sommer, "Analogue models - Veins github," https://github.com/sommer/veins/tree/master/src/veins/modules/analogueModel, accessed: 2025-05-01.